Multi-modal weighted quadratic priors for robust intensity independent synergistic PET-MR reconstruction

I. Introduction

The simultaneous and co-registered acquisition of PET and MR data in a simultaneous PET-MR scanner provides opportunity for the reconstruction of PET and MR data using synergistic methods which improve the quality of reconstructed images beyond what would be currently achieved by conventional separate reconstruction methods. In synergistic reconstruction, the common features of PET and MR images, such as anatomical and physiological boundaries, are exploited to reconstruct PET-MR images from low-count PET data and/or highly under-sampled MRI data. The major challenges encountered in joint PET-MR reconstruction are the development of i) a model-based joint prior that favors the common features between PET and MR images, irrespective of their relative signal intensities and their relative contrast orientations while preserving modality unique features, and ii) a robust and stable optimization algorithm with preferably few hyper-parameters, controlling the overall performance of the algorithm. Ehrhardt *et al* [1] reported the first attempt in joint PET-MR image reconstruction based on the parallelism of PET-MR level sets (PLS), while Knoll *et al* [2] proposed a nuclear norm-based total generalized variation regularization for joint PET-MR reconstruction. Despite promising results, their methods potentially depend on the signal intensity and edge orientation. In [3], we recently proposed a total variation (TV) prior generalized using a non-convex potential function together with an alternating scaling scheme to handle the intensity differences between PET and MR images. The results showed that the proposed prior can outperform the PLS and joint TV priors, however, the proposed scaling scheme was designed such that it globally matches the magnitude of PET and MR image gradients, therefore it might not be efficient for all regions in the images. In [1], PET-MR images were reconstructed simultaneously using a quasi-Newton method, whose convergence depends on the initial guess. In [2] and [3], a first-order primal-dual algorithm and an alternating direction method of multipliers (ADMM) were employed respectively. These algorithms aim to break down the problem into simpler sub-problems and estimate images in an alternating fashion. However, they introduce additional hyper-parameters that need to be chosen properly. In this study, we aimed to propose a simple, robust and clinically feasible synergistic reconstruction framework with dual-modal quadratic priors (readily extendable to multi-modal priors) which are independent of the signal intensity and contrast orientation of the PET-MR images. It this study, we present out preliminary results using realistic 3D simulations and a clinical PET-MR dataset.

II. Material and methods

A. Joint reconstruction algorithm

In joint PET-MR reconstruction, we aim to maximize the following objective function:

$$(\hat{\boldsymbol{u}},\hat{\boldsymbol{v}}) = \underset{\boldsymbol{u}\in\mathbb{R}^{N_u},\boldsymbol{v}\in\mathbb{C}^{N_v}}{\operatorname{argmax}} \{\mathcal{D}_u(\boldsymbol{Pu},\boldsymbol{y}) + \mathcal{D}_v(\boldsymbol{Ev},\boldsymbol{s}) + R(\boldsymbol{u},\boldsymbol{v})\} \tag{1}$$

where $\boldsymbol{u}$ and $\boldsymbol{v}$ are PET and MR images discretized by N_u and N_v voxels, $\boldsymbol{y}\in\mathbb{R}^{M_u}$ and $\boldsymbol{s}\in\mathbb{C}^{M_vL}$ are PET sinogram data and MR multi-channel k-space data with L channels, $\boldsymbol{P}\in\mathbb{R}^{M_u\times N_u}$ is the PET system matrix and $\boldsymbol{E}\in\mathbb{C}^{M_vL\times N_v}$ is the MR Fourier encoding matrix, $\mathcal{D}_u$ and $\mathcal{D}_v$ are respectively PET and MR data fidelity terms defined as:

$$\mathcal{D}_u(\boldsymbol{Pu},\boldsymbol{y}) = \sum_{i=1}^{M_u}(\boldsymbol{y}_i\log([\boldsymbol{Pu}]_i + \bar{\boldsymbol{r}}_i) - [\boldsymbol{Pu}]_i - \bar{\boldsymbol{r}}_i) \tag{2}$$

$$\mathcal{D}_v(\boldsymbol{Ev},\boldsymbol{s}) = -\sum_{l=1}^{L}\sum_{i=1}^{M_v} w_{li}([\boldsymbol{Ev}]_{li} - \boldsymbol{s}_{li})^2 \tag{3}$$

where $\bar{\boldsymbol{r}}$ are expected random and scatter coincidences during PET acquisition. In this study, the joint prior R was defined as two quadratic priors weighted by some joint weighting coefficients, ω, as follows:

$$R(\boldsymbol{u},\boldsymbol{v}) = \frac{\beta_u}{2}\sum_{j=1}^{N_u}\sum_{k\in\mathcal{N}_j}\xi^u_{jk}\omega^u_{jk}(u_j-u_k)^2 + \frac{\beta_v}{2}\sum_{j=1}^{N_v}\sum_{k\in\mathcal{N}_j}\xi^v_{jk}\omega^v_{jk}(v_j-v_k)^2 \tag{4}$$

where ξ_{jk} and ω_{jk} are respectively weighting coefficients that weight differences between voxel j and u based on their Euclidean proximity and intensity similarity in a neighbourhood $\mathcal{N}_j$. βs are regularization parameters. In the proposed method, the similarity coefficients are alternatively calculated from both PET and MR images using the following joint coefficients, inspired from joint Burg entropy prior [4]:

$$\omega_{jk} = \frac{\mathcal{G}(u_j,u_k,\sigma_u)\mathcal{G}(v_j,v_k,\sigma_v)}{\sum_{j=1}^{N}\mathcal{G}(u_j,u_k,\sigma_u)\mathcal{G}(v_j,v_k,\sigma_v)} \tag{4}$$

$$\mathcal{G}(q,r,\sigma) = \frac{1}{\sqrt{2\pi}\sigma}\exp\left(-\frac{(q-r)^2}{2\sigma^2}\right)$$

where the joint coefficients encourage formation of joint boundaries by suppressing the regularization across them. The reconstruction algorithm can be summarized follows:

Algorithm 1:
Initialize $\omega^u_{jk} = \boldsymbol{1}$, $\omega^v_{jk} = \boldsymbol{1}$, σ_u, σ_v, β_u, β_v, $\boldsymbol{u}^0$, $\boldsymbol{v}^0$

1. Maximum *a posteriori* (MAP) PET reconstruction using DePierro's method.

1a. Conventional expectation maximization (EM) update:

$$\boldsymbol{u}^{n+1}_{EM} = \frac{\boldsymbol{u}^n}{\boldsymbol{P}^T\boldsymbol{1}}\boldsymbol{P}^T\left(\frac{\boldsymbol{y}}{\boldsymbol{Pu}^n + \bar{\boldsymbol{r}}_i}\right) \tag{5}$$

1b. Regularization:

$$u^{n+1}_j = \frac{2s_j u^{n+1}_{EM,j}}{B + \sqrt{B^2 + 4\beta_u s_j u^{n+1}_{EM,j}\sum_{k\in\mathcal{N}_j}\xi^u_{jk}\omega^u_{jk}}} \tag{6}$$

$$B = s_j - \frac{\beta_u}{2}\sum_{k\in\mathcal{N}_j}\xi^u_{jk}\omega^u_{jk}\left(u^n_j + u^n_k\right), \qquad s_j = \sum_i p_{ij}$$

2. MAP MR reconstruction using the conjugate gradient (CG) algorithm, initialized by $\boldsymbol{v}^n$ to iteratively arrive at the solution $\boldsymbol{v}^{n+1}$ that satisfies, where $\boldsymbol{D}$ is a derivative matrix:

$$(\boldsymbol{E}^H\boldsymbol{WE} + \beta_v\boldsymbol{D}^T\boldsymbol{\xi}^v\boldsymbol{\omega}^v\boldsymbol{D})\boldsymbol{v}^{n+1} = \boldsymbol{E}^H\boldsymbol{Ws} \tag{7}$$

3. Update the joint weighting coefficients:

3a. Map the current MR estimate into PET space, $\bar{\boldsymbol{v}}^{n+1} \leftarrow \boldsymbol{\Phi}_v\boldsymbol{v}^{n+1}$, and calculate ω^u_{jk}

$$\omega^u_{jk} = \frac{\mathcal{G}(u^{n+1}_j,u^{n+1}_k,\sigma_u)\mathcal{G}(\bar{v}^{n+1}_j,\bar{v}^{n+1}_k,\sigma_v)}{\sum_{j=1}^{N_u}\mathcal{G}(u^{n+1}_j,u^{n+1}_k,\sigma_u)\mathcal{G}(\bar{v}^{n+1}_j,\bar{v}^{n+1}_k,\sigma_v)} \tag{8}$$

3b. Map the current PET estimate into MR space, $\bar{\boldsymbol{u}}^{n+1} \leftarrow \boldsymbol{\Phi}_u\boldsymbol{u}^{n+1}$, and calculate ω^v_{jk}

$$\omega^v_{jk} = \frac{\mathcal{G}(\bar{u}^{n+1}_j,\bar{u}^{n+1}_k,\sigma_u)\mathcal{G}(v^{n+1}_j,v^{n+1}_k,\sigma_v)}{\sum_{j=1}^{N_v}\mathcal{G}(\bar{u}^{n+1}_j,\bar{u}^{n+1}_k,\sigma_u)\mathcal{G}(v^{n+1}_j,v^{n+1}_k,\sigma_v)} \tag{9}$$

B. Simulations and clinical data

The BrainWeb phantom was used to simulate an FDG activity distribution and a T1-weighted MR phantom with the matrix sizes of 344×344×127 and 148×148×127 and voxels of size 2.086×2.086×2.03 mm^3. 3D realistic simulations were performed for the native geometry of the Siemens Biograph mMR scanner including attenuation, normalization factors, 10% randoms and 35% scatter coincidences with 90 million counts. MR simulations were performed for a 5-channel scan with Cartesian undersampling factors (R) of 4, 6 and 8 in the phase encoding direction of k-space, contaminated by complex Gaussian noise. A clinical brain PET-MR scan was acquired on the mMR scanner for a 214.7 MBq injection of [^{18}F]FDG for a 30-minute PET scan. T1-weighted and FLAIR MR acquisitions were performed on the 3T MRI subsystem of the scanner using the 5-channel head and neck coil array. The PET images were reconstructed with matrix size of 344×344×127 and voxel size of 2.086×2.086×2.03 mm^3 while fully and undersampled T1-MR images were reconstructed with matrix size of 404×244×244 and voxel size of 1.05×1.05×1.1 mm^3. The fully-sampled T1 images were used as a MR benchmark, also to anatomically guide the reconstruction of PET images, as PET benchmark. The fully-sampled FLAIR MR images were also used to anatomically guide reconstruction of undersampled T1 MR images (with R = 4).

III. Results

Fig. 1 shows the results of simulations for different PET and MR reconstruction methods and MR undersampling factors. PET reconstruction methods include: maximum-likelihood expectation maximization (MLEM), MLEM with 4 mm post-reconstruction Gaussian smoothing, MR-guided MAPEM with Gaussian coefficients ($\mathcal{G}$) derived from fully-sampled MR image and synergistic reconstruction. MR reconstruction methods include: MR sensitivity encoding (SENSE) reconstruction using fully-sampled data, and undersampled data. The undersampled data were also reconstructed using TV regularization, PET-guided SENSE (for which Gaussian weighting coefficients derived from ground truth PET were used to guide the reconstruction) and the proposed synergistic reconstruction method.

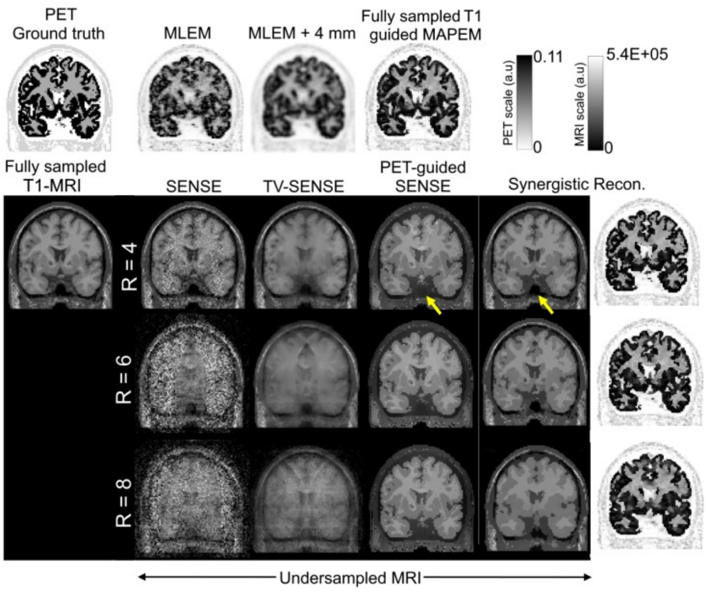

Fig. 1. Simulation results for the included PET and MR reconstruction methods for different MR undersampling factors (R).

As shown, for PET reconstruction the proposed synergistic method achieves an image quality comparable to the benchmark MR-guided MAPEM method, even using MR data undersampled as much as 6 times. For MR reconstruction, as the undersampling factor is increased, noise and undersampling artifacts dominate the MR images. The results show that TV regularization, optimized using an ADMM algorithm, is not able to remove the aliasing artifacts and recover the lost tissue contrast. The PET-guided MR reconstruction results in a notable reduction of artifacts and recovery of structures, however, it suppresses some features of MR that are absent in PET, for example the spinal canal at the mid-base of the brain (see arrows). For synergistic reconstruction, our results show that as the undersampling factor is increased, the quality of reconstructed images is reduced, nonetheless, the proposed method outperforms the conventional separate reconstruction and even in the case of PET-MR mismatches, it outperforms the PET-guided SENSE method (see arrows). The preservation of modality-unique features should be attributed to the fact that the Gaussian weighting coefficients are jointly derived from both PET and MR images. In Fig. 2, an example of the summed-coefficients of the MR reconstruction is shown. Note they are shown before normalization to 1. Table 1 also summarizes the quantitative performance of the methods based on the normalized root mean square error (NRMSE) between the reconstructed images are their ground truth images calculated over the brain tissue (white and grey matter). The results show that for PET and MR reconstruction, the MR-guided MAPEM and the proposed synergistic method results in the best NRMSE performance.

Fig. 3 shows the reconstruction results of the clinical dataset for the same methods as our simulations. For these preliminary results, we consider an MR undersampling factor of 4 and used the FLAIR image to guide the MR reconstruction as the MLEM PET images are of lower resolution and have less structural detail. As shown, in terms of boundary definition and overall

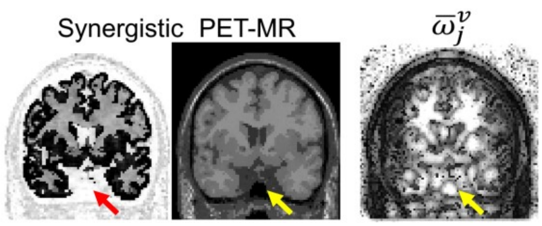

Fig. 2. The joint coefficients calculated for MR recon according to Eq. (9) summed without normalization, $\overline{\omega}_j^v = \sum_{k\in\mathcal{N}_j} \omega_{jk}^v$, showing MR unique features are captured and ultimately preserved.

Table 1. NRMSE (%) for the reconstructed methods in brain tissues (grey and white matters) and different MR undersampling factors (R).

Methods	Modality					
			PET			
MLEM			30.0			
MLEM+4mm			35.0			
MR-guided MAPEM			16.0			
			MRI			
	R = 4		*R = 6*		*R = 8*	
SENSE	12.1		22.5		25.4	
TV-SENSE	8.7		13.5		14.7	
PET-guided SENSE	8.9		8.3		7.2	
			PET-MR			
	R = 4		*R = 6*		*R = 8*	
Synergistic Recon.	PET	MR	PET	MR	PET	MR
	18.8	4.4	21.0	5.7	24.1	6.9

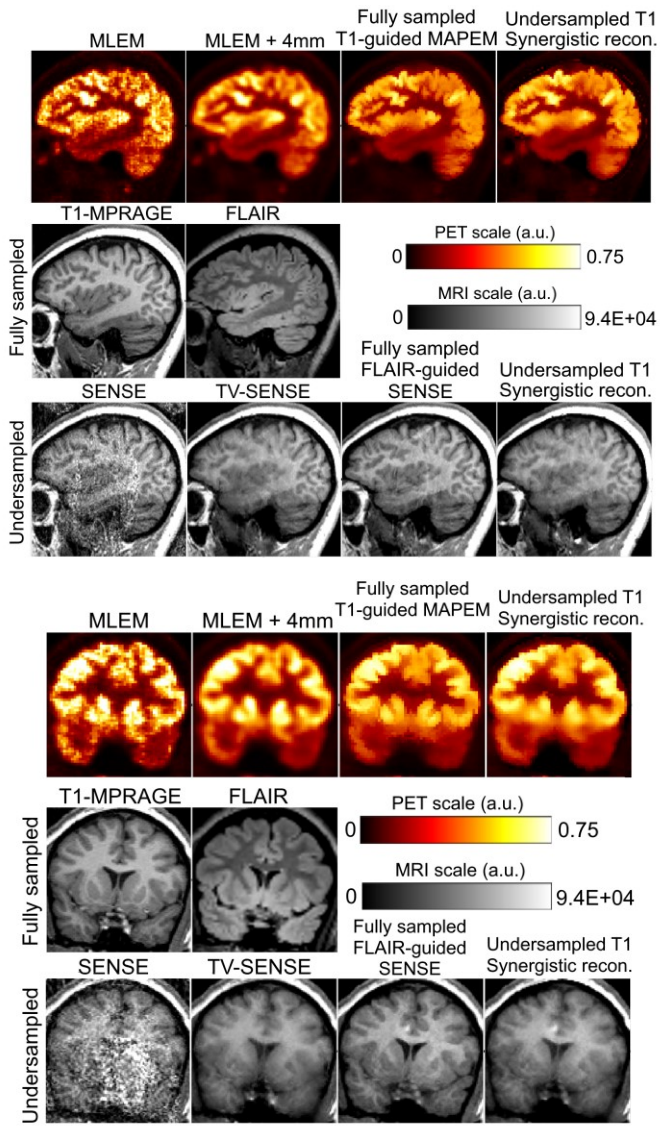

Fig. 3. Clinical results for the different methods, for an MR undersampling factor of 4.

qualitative image quality, the T1-guided PET and FLAIR-guided MR reconstruction achieve the best results. In contrast to our simulation results, our current clinical results show that the benefits of the proposed method is more pronounced for PET reconstruction than the MR reconstruction, since the synergistically reconstructed PET images are more comparable to the T1-guided PET images, while the synergistically reconstructed MR images are comparable to the TV-SENSE results. This can be largely ascribed to the sub-optimal selection of the MR hyper-parameters. In addition, for greater undersampling factors the different between separate and synergistic reconstruction should be more pronounced. Future work will include the hyper-parameter selection and investigating greater MR undersampling factors.

IV. Conclusion

In this study, a simple and robust algorithm was proposed for multi-modal synergistic reconstruction of PET and MR images using jointly-weighted quadratic priors. Both simulation and clinical results showed the proposed priors are insensitive to the signal intensity and contrast differences between PET and MR images. In addition, it was found that these priors can preserve PET or MR unique features. In conclusion, our results showed that the proposed synergistic algorithm and priors are promising for multi-modal synergistic reconstruction in simultaneous PET-MR systems.

Acknowledgements

This work is supported by engineering and physical sciences research council (EPSRC) under grant EP/M020142/1.

References

[1] M. J. Ehrhardt, K. Thielemans, L. Pizarro, D. Atkinson, S. Ourselin, B. F. Hutton, et al., "Joint reconstruction of PET-MRI by exploiting structural similarity," Inverse Problems, vol. 31, Jan 2015.

[2] F. Knoll, M. Holler, T. Koesters, R. Otazo, K. Bredies, and D. Sodickson, "Joint MR-PET reconstruction using a multi-channel image regularizer," IEEE Tran Med Imaging, vol. PP, pp. 1-1, 2016.

[3] A. Mehranian, M. Belzunce, C. Prieto, A. Hammers, and A. Reader, "Synergistic PET and SENSE MR image reconstruction using joint sparsity regularization," IEEE Trans Med Imaging, Apr 18 2017.

[4] A. Mehranian and A. J. Reader, "Multi-parametric MRI-guided PET image reconstruction," presented at the IEEE Nuclear Science Symposium and Medical Imaging Conference, 2016.